Biosensors and Bioelectronics 68 (2015) 115–121

Contents lists available at ScienceDirect

Biosensors and Bioelectronics

journal homepage: www.elsevier.com/locate/bios

Gelsolin bound β-amyloid peptides$_{(1-40/1-42)}$: Electrochemical evaluation of levels of soluble peptide associated with Alzheimer's disease

Yanyan Yu [a,b,1], Xiaoyu Sun [b,1], Daoquan Tang [a,b], Chenglin Li [b], Lin Zhang [b], Dongxia Nie [c], Xiaoxing Yin [b,*], Guoyue Shi [d,**]

[a] Department of Pharmaceutical Analysis, Xuzhou Medical College, 209 Tongshan Road, Xuzhou 221004, PR China
[b] Jiangsu Key Laboratory of New Drug Research and Clinical Pharmacy, Xuzhou Medical College, 209 Tongshan Road, Xuzhou 221004, Jiangsu, PR China
[c] Institute of Agro-food Standards and Testing Technologies, Shanghai Academy of Agricultural Sciences, 1000 Jinqi Road, Shanghai 201403, PR China
[d] Department of Chemistry, East China Normal University, 500 Dongchuan Road, Shanghai 200241, PR China

ARTICLE INFO

Article history:
Received 16 October 2014
Received in revised form
15 December 2014
Accepted 17 December 2014
Available online 18 December 2014

Keywords:
$A\beta_{1-40/1-42}$
Gelsolin
Electrochemistry
AD

ABSTRACT

A method for the highly sensitive determination of soluable β-amyloid peptides ($A\beta_{1-40/1-42}$) that employs a detection bioconjugate of HRP–Au–gelsolin as the electrochemical nanoprobe is presented. Contrary to previous detection notions that utilized antibodies, which could specifically recognize the N- or C-terminus of peptides, we demonstrate herein that the reported specific binding between gelsolin and Aβ might provide an alternative way to evaluate the peptides sensitively and selectively. The HRP–Au–gelsolin nanohybrid was designed by one-pot functionalization of Au nanaoparticles (NPs) with horseradish peroxidase (HRP) and gelsolin. Through a sandwich-type sensor array, soluble $A\beta_{1-40/1-42}$ were captured onto the array due to the interactions between targeted peptides and surface-confined gelsolin and electrochemical signals were amplified by abundant attachments of HRP labeled on AuNPs, which could specifically catalyse its substrate, 3,3′,5,5′-tetramethylbenzidine (TMB) in the presence of H_2O_2 to give rise to measurable signals. The proposed gelsolin-bound Aβ methodology displayed satisfactory sensitivity and wide linear range towards $A\beta_{1-40/1-42}$ with a detection limit down to 28 pM, which are verified to be sensitive-enough for the assessment of Aβ levels both in normal and Alzheimer's disease (AD) rat brains. Experimental results indicated that compared with normal group, soluble β-amyloid peptide levels in cerebrospinal fluid (CSF) and targeted brain tissues of AD rats all declined with differentiable degrees. In short, the newly unfolding strategy presents valuable information related to pathological events in brain and will exhibit a braw perspective for the early diagnosis of AD process.

1. Introduction

Alzheimer's disease (AD), an age-related neurodegenerative condition, was associated with an early impairment in memory and was the major cause of dementia in the elderly (Jiang et al., 2013). As the most common neurodegenerative disease, it has been estimated an increase of up to 106.8 million people by 2050 (Yang et al., 2013). The main characteristic features of AD include gradual loss of cognitive function and synaptic integrity, selective neuronal death and abnormal formation of neurotic and core plaques in the cerebral cortex (Hardy and Selkoe, 2002; Liu et al., 2014). However, so far, no effective treatment for this neurodegenerative disorder has been found and developed.

The pathological features of AD include extracellular neuritic plaques containing β-amyloid peptide (Aβ) and intracellular neurofibrillary tangles (NFTs), which are composed of hyperphosphorylated microtubule-associated protein tau. Experimental data from both *in vitro* and *in vivo* studies have indicated that aggregated Aβ initiate a pathogenic cascade that ultimately leads to neuronal loss and dementia (Glenner and Wong, 1984). Amyloid associated with Alzheimer's disease consists of thin fibrils of polymerized Aβ with an ordered β-sheet pattern in AD brains (Ranjini et al., 2012). The actual form of Aβ that causes the damage is most likely a small dimeric or higher oligomeric species with internal β-sheet structure (Selkoe, 1996). Aβ variants, such as $A\beta_{1-40}$ and $A\beta_{1-42}$, are produced by sequential cleavage of APP by β- and γ-secretases. Inhibitors of β- or γ-secretase or modulators of γ-secretase result in the lowering of central $A\beta_{1-40}$ and $A\beta_{1-42}$ levels and are therefore pursued as potential disease modifying treatments for AD (Citron, 2010; Niva et al., 2013). Therefore, the

* Correponding author. Fax: +86 516 8326 2630.
** Correponding author. Fax: +86 21 5434 0043.
E-mail addresses: yinxx@xzmc.edu.cn (X. Yin), gyshi@chem.ecnu.edu.cn (G. Shi).
[1] These authors contributed equally to this work.

http://dx.doi.org/10.1016/j.bios.2014.12.041
0956-5663/

two Aβ variants are nowadays widely believed to be important biomarkers and drug targets for AD research and therapy.

Under such circumstance, with the development of amyloid-sensitive ligands, new approaches aimed at assessing amyloid plaque aggregation are thus developed to lessen the burdens of both society and family, including methods that indirectly estimate levels of brain amyloid plaques from Aβ levels in plasma or cerebral spinal fluid (CSF) (Rodrigue et al., 2009). However, most of these methods belong to postmortem identifications, which are often inevitably influenced by the age of the cohort sampled and the method of defining disease pathology (Bennett et al., 2006; Thal et al., 2006). Currently, biochemical assays such as polyacrylamide gel electrophoresis (PAGE), immunoprecipitation, enzyme-linked immunosorbent assay (ELISA) and also non-biochemical techniques, incluindg surface plasmon resonance (SPR), mass spectrometry, capillary electrophoresis have been employed to detect Aβ species from body fluids and cell media (Xia et al., 2010; Golde et al., 2000; Munishkina and Fink, 2007; Picou et al., 2010). Although high sensitivity, selectivity and reliability of ELISA seems more attractive, inherent shortcomings of this technique such as relatively expensive enzyme-linked antibody for Aβ recognition and carcinogenic substrate for chemiluminescent detection should not be ignored. Alternatively, electrochemical biosensors have been considered as a promising technique because of their simplicity, rapid response, and potential ability for real-time and on-site analysis (Zhang et al., 2008), which are typically labeld with an electroactive species to generate corresponding electrochemial signals. Hence, labels that are designed for signal amplification have always been a favorable candidate in the biosensor fabrication, including functionalized liposomes, enzymes and various nanomaterials (Yu et al., 2006; Lu et al., 2008). For example, Liu and co-workers presented a sensitive and selective electrochemical immunosensor for the detection of both $A\beta_{1-42}$ and total Aβ using p-AP redox cycling by tris (2-carboxyethyl) phosphine (Liu et al., 2014), which achieved a low detection limit of 5 pM for $A\beta_{1-42}$ and this value was comparable or even lower than other non-electrochemical methods.

Discovery of strong interactions between two completely different proteins led to suggestions that the specific affinity could be employed in a similar way as antibody–antigen interaction and hence develop a novel methodology for the detection of one of these proteins. Compared with other detection strategies, this notion emblems no complicated substances or chemical bonds that would be invovled to capture Aβ and therefore becomes much easier to perform. In 1999, Chauhan's group has found that a secretory protein named gelsolin, can bind to soluable Aβ peptide in a concentration-dependent manner (Chauhan et al., 1999). It was found that more gelsolin was taken, more Aβ would be bound until the binding reached the saturation and more significantly, this specificity was proved to be applicable for both $A\beta_{1-40}$ and $A\beta_{1-42}$ monomers, not their oligomeric and fibril forms. Since $A\beta_{1-40}$ and $A\beta_{1-42}$ possess more significance toward AD occurance and development in human, this specific binding between $A\beta_{1-40/1-42}$ and gelsolin, somewhat like the interaction between antibody and antigen, would be applicable to fabricate a novel electrochemical immunoassay for the detection of total amount of $A\beta_{1-40}$ and $A\beta_{1-42}$.

Herein, on the basis of our previous work, we reported the design and evaluation of an alternative approach for electrochemical protein assay employing platforms featuring well-dispersed Au nanoparticles (NPs). The specific recognition of our target, $A\beta_{1-40/1-42}$ was achieved using gelsolin that can specifically bind to $A\beta_{1-40/1-42}$, as the recognition element for further insight into the floating of Aβ levels in the process of AD. Accordingly, a nanohybrid of HRP–Au–gelsolin was prepared by one-pot in situ functionalization of AuNPs with HRP and gelsolin and used as the detection probe to capture $A\beta_{1-40/1-42}$. Signal amplification was achieved *via* enormous loading of HRP on the AuNPs and its strong catalytic activity towards its substrate TMB to produce measurable redox currents. The results indicated that the established gelsolin-based electrochemical assay possesses resonable sensitivity and selectivity, which has met the requirement of evaluating dynamic changes of $A\beta_{1-40/1-42}$ levels in CSF, brain tissues of both normal and AD rats.

2. Materials and methods

2.1. Chemicals and materials

Gelsolin protein from human source was purchased from Qcbio Science and Technologies Co., Ltd. (Shanghai, China) and dissolved in 25 mM Tris–HCl (pH 7.5). Purified synthetic β-amyloid peptides ($A\beta_{1-40}$ and $A\beta_{1-42}$) were obtained from ChinaPeptides Co,. Ltd. (Shanghai, China). Horseradish peroxidase (HRP) and 3,3′,5,5′-tetramethylbenzidine (TMB) were from Sigma Co. Chloroauric acid ($HAuCl_4 \cdot 4H_2O$) was purchased from Sinopharm Chemical Reagent Co., Ltd. Multi-walled carbon nanotubes (MWCNTs) were from Chengdu Institute of Organic Chemistry Nanotech Port Co., Ltd. (Chengdu, China). 1-ethyl-3-[3-dimethylaminopro-pyl]carbodiimide hydrochloride (EDC), N-hydroxysulfosuccinimide (NHS), and bovine serum albumin (BSA) were obtained from from J&K Scientific, Ltd. Phosphate buffer saline (PBS, pH 7.4) containing 8.72 mM Na_2HPO_4, 1.41 mM KH_2PO_4, 136.7 mM NaCl and 2.7 mM KCl was employed as incubation buffer. The washing buffer was PBS (0.1 M, pH 7.4) containing 0.05% (w/v) Tween-20 (PBST). Blocking buffer was 1% (w/v) BSA containing 0.05% Tween-20. Water (≥ 18 MΩ) used throughout the whole experiment was purified with Millipore system. All reagents were of the analytical grade commercially available and used without further purification.

2.2. Instruments

UV–vis absorption characterizations were performed on a UV–vis 2450 spectrometer (Shimadzu, Japan). The size distribution and dispersing behaviors of AuNPs and the prepared HRP–Au–gelsolin were measured by using a FEI Tecnai G2 T12 transmission electron microscope (TEM, USA) operating at 120 kV. The TEM specimens were prepared by dropping the sample solutions onto 50 Å carbon coated copper grids with the excess solution being immediately wicked away. All the electrochemical experiments were carried out on CHI 832 electrochemical workstation (CHI Company, China). A conventional three-electrode system through the experiments composed of a platinum wire as counter electrode, a saturated calomel electrode (SCE) (Jiangsu Electroanalytical Instruments Factory, China) as reference electrode, and a bare or a modified glassy carbon electrode (GCE) as working electrode.

2.3. Preparation of HRP–Au–gelsolin bioconjugate

AuNPs with an average diameter of 20 nm were prepared as follows: to a boiling and rapidly stirred $HAuCl_4$ solution (0.01%, 250 mL), 3.75 mL trisodium citrate solution (1%) was added. The color of the solution turned from pale yellow to deep purple within 2 min. After that, the mixture was kept boiling, stirred for 15 min and cooled to room temperature to obtain AuNPs. For the preparation of the bioconjugate, 40 μL of 10 mg/mL HRP and 20 μL of 0.2 mg/mL gelsolin were added to 0.5 mL of AuNPs. The mixed solution was gently mixed for 3 h with 140 rpm at 25 °C and centrifuged at 3500 rpm for 15 min at 4 °C. The supernatant was discarded and the obtained bioconjugate was washed with PBST

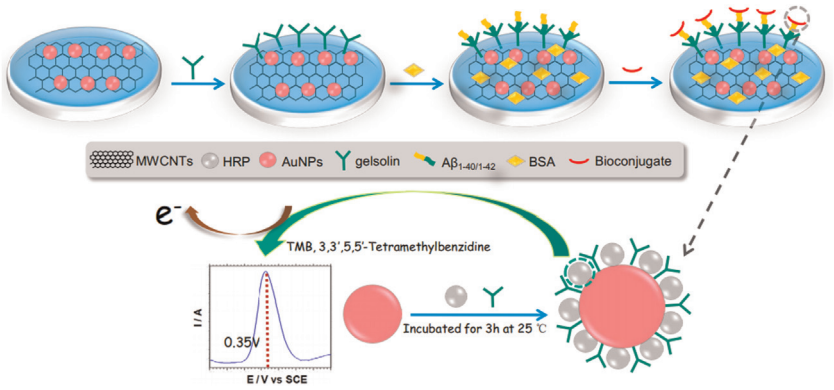

Scheme 1. Presentation of the gelsolin-bound electrochemical method for the sensing of $A\beta_{1-40/1-42}$ in normal and AD rats.

and resuspended in 500 μL PBS (pH 7.4) containing 0.04% BSA. The obtained bioconjugates solution was stored in a refrigerator at 4 °C until use. To acquire the optimized bioconjugate, different ratios of HRP to gelsolin were tested during preparation.

2.4. Fabrication of gelsolin-bound-$A\beta_{1-40/1-42}$ detection assay

Before modification, the bare glassy carbon electrode (GC) was pre-cleaned using acetone, ethanol and distilled water with ultrasonication. As shown in Scheme 1, firstly, 5 μL of MWCNTs-DMF suspension (0.5 mg/mL) was dropped onto the cleaned sensor surface. After air-dried for 20 min and washed with distilled water, 10 μL of the prepared AuNPs solution was applied to the center of working electrode, dried for 2 h, followed by activation with EDC/NHS for 2 h and washed with distilled water. Subsequently, 0.5 μL of 0.2 mg/mL gelsolin dissolved in Tris–HCl solution (25 mM, pH 7.5) was casted onto the formed MWCNT–AuNPs film and dried for 6 h. Following that, the resulting sensor was washed thrice with PBS and PBST to remove the physically adsorbed proteins. Then, a drop of 10 μL blocking solution was applied to the assay to eliminate the non-specific binding effects and block the remaining active sites. After another washing cycle with PBS and PBST, the finished sensor was stored in 4 °C when not in use.

In this assay, the detection principle of Aβ was based on the "sandwich" strategy. Firstly, the prepared MWCNTs–AuNPs–gelsolin sensor was incubated with a 10 μL drop of the mixture of $A\beta_{1-40}$ and $A\beta_{1-42}$ standard aqueous solutions (6:1, close to the real ratio in rat brain) with different concentrations or real samples overnight in a moisture-satuated condition at 37 °C, followed by washing with PBS and PBST for three times. It was then incubated in 10 μL of the prepared HRP–Au–gelsolin bioconjugate for 6 h at room temperature. After rinsing throughly with PBS and PBST to remove the unbound bioconjugate, the amperometric responses of the resultant sensor were recorded with TMB as the peroxidase substrate by differential pulse voltammetry (DPV) technique for the quantitative detection of total amount of $A\beta_{1-40}$ and $A\beta_{1-42}$.

3. Results and discussion

3.1. Detection principle

For the sensor fabrication, a nanoplatform featuring MWCNTs and densely packed AuNPs was employed, which was easy to process and can be pre-equipped with a functional organic layer for capturing protein. We then attached the capture protein, gelsolin onto the MWCNTs/AuNPs platform for the determination of Aβ in standard solutions or rat brains through the specific binding between gelsolin and Aβ. Highly amplified detection was achieved by incubation of the above sensor with the multi-labeled bioconjugates prepared by linking multiple HRP and gelsolin to AuNPs for signal development. The HRP on the bound bioconjugates could catalyze TMB in the presence of H_2O_2 and produce a visible reduction current at +0.35 V on the sensor surface. The peak current was directly related to the amount of HRP on the sensor and therefore, reflected the actual amount of targeted Aβ species in rat brains, providing a strategy for the dynamic monitoring of Aβ levels associated with AD process.

3.2. Analytical performance of the fabricated sensor

The step-by-step fabrication was characterized by UV–vis and TEM (Fig. S1) as well as electrochemical techniques. Fig. S3 displayed the current change of the sensor layer-by-layer assembly in $K_3Fe(CN)_6$ solution. Clearly observed in panels a–f, densely packed MWCNTs and subsequent AuNPs layers (b, and c) contributed to the enhancement of charging currents compared with that on bare electrode (a) due to the excellent conductivity and electrochemical acitivity. Additionally, the binding of gelsolin and the capture of Aβ to MWCNTs/AuNPs modified sensor hindered the access of the redox probe to the sensor, leading to an obviously gradual decrease in the produced currents because of the massive loading of poorly-conductive proteins (d, and e). However, when the as-prepared bioconjugate was dropped onto the sensor, the current became larger again because of the contribution of the assembled AuNPs existing in the bioconjugate (f). The important role of MWCNTs and AuNPs can be further confirmed by DPV technique. Curves a, b, c in Fig. 1A represent the DPV profiles on AuNPs, MWCNTs and MWCNTs/AuNPs modified electrodes in the same Aβ solution, respectively. It was obvious that the highest current was produced on MWCNTs/AuNPs modified electrode, with almost three times as high as that on AuNPs-modified electrode, indicating the facilitated electron transfer rate of MWCNTs and AuNPs. As indicated from the above results, the highly conductive MWCNTs/AuNPs composite not only acted as an effective matrix for gelsolin capture and retaining its original bioactivity, but also greatly enhanced the electrical connectivity, which improved the sensitivity of Aβ detection in rat brain. This result also demonstrated that our strategy that employing MWCNTs and AuNPs as the electrode substrate was feasible and necessary for constructing a sensitive biosensor capable of determining low Aβ peptide concentration in biological matrix.

3.3. Specific recognition of the HRP–Au–gelsolin bioconjugate to

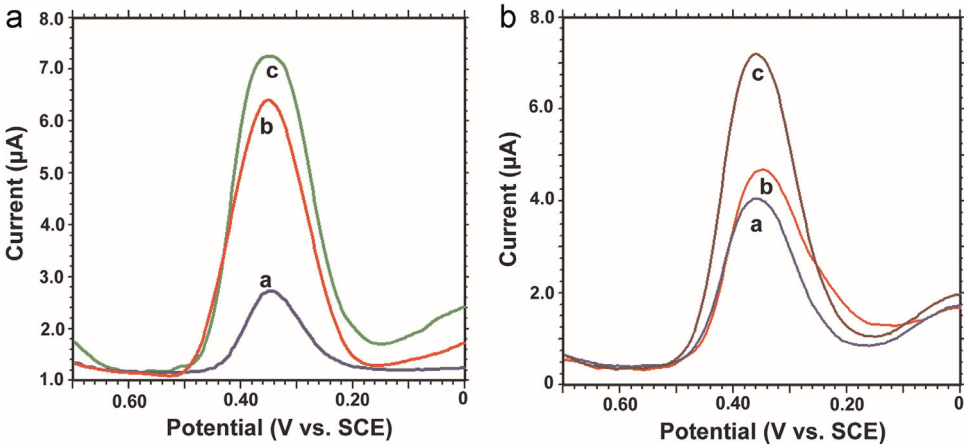

Fig. 1. (A) Comparison of DPV responses toward 20 nM $A\beta_{1-40/1-42}$ standard solution employing AuNPs (a), MWCNTs (b) and MWCNTs/AuNPs (c) as the sensor substrates. (B) Illustration of the specific recognition of HRP–Au–gelsolin conjugate to $A\beta_{1-40/1-42}$ standard solution. DPV responses for 20 nM $A\beta_{1-40/1-42}$ after incubation with (a) first gelsolin and then HRP–Au–gelsolin bioconjugate, (b) a mixture of gelsolin and HRP–Au–gelsolin conjugate and (c) HRP–Au–gelsolin conjugate.

$A\beta_{1-40/1-42}$

The specific binding of gelsolin to soluble $A\beta_{1-40}$ and $A\beta_{1-42}$ was firstly reported by Chauhan's group in 1999. In our previous work, this association was also successfully reproduced and detailed discussed *via* the immunoprecipitation (IP) *in vitro* and *in vivo,* protein docking and molecular dynamics simulation techniques (Yu et al., 2014). Since the current signals were produced *via* the catalysis of TMB by HRP entrapped in the bioconjugate, assuming the concentration of TMB kept constant through the whole experiment, any factor that was not in favor of the adhesion and binding of the bioconjugate to Aβ would influence the final signal production. Consequently, two experiments as for blocking and competitive electrochemical experiments were performed, which were done by initial incubation of Aβ with gelsolin and the follow-up HRP–Au–gelsolin conjugate denoted as blocking experiment, and coating the mixture of gelsolin and HRP–Au–gelsolin conjugate in one step to incubate the MWCNTs/AuNPs/gelsolin/Aβ sensor named as competitive experiment, respectively. As shown in Fig. 1B, both of the two situations witness an obvious decrease in the reduction currents in comparison with that on the electrodes fabricated in the regular way (curve c). The initial incubation of Aβ with gelsolin and then the bioconjugate resulted in the occupation of binding sites on Aβ (curve a), as well as the efficient competition between dissociative gelsolin and bound HRP–Au–gelsolin (curve b), all prevented binding of the bioconjugate to Aβ and the decrease of the amount of HRP and thus a visual decrease in current responses was obtained. These results also confirmed the existance of specific interaction between gelsolin and Aβ. It should be emphasized herein that up to now, a variety of electrochemical strategies focusing on the specific $A\beta_{1-40}$ or $A\beta_{1-42}$ detection were mostly carried out by employing their corresponding monoclonal antibodies in combination with complex chemical bonds to capture Aβ onto sensors (Liu et al., 2013, 2014; Rama et al., 2014). However, in this work, for the first time, this specificity can be readily realized by linking an acquirable protein (gelsolin) onto the sensor due to their interactions similar to antibody–antigen, which was much easier to understand and handle than those similar methods.

3.4. Optimization of detection conditions

To acquire a satisfactory detection sensitivity, optimizations for some key parameters should be concerned. First of all, by keeping the experimental conditions for the detection step the same but increasing the concentration of gelsolin (from 0.05 to 1.0 mg/mL), we were able to observe the continuous changes in the tested range and found that the current responses toward 20 nM Aβ rapidly increased at the beginning and reached the maximum at the concentration of 0.2 mg/mL. Afterwards, the responses began to gradually level off (Fig. 2A). The foregoing signal enhancement could be ascribed to the elevatory amount of captured targets and thus contributed to the increase in the detection conjugate whereas the decrease in the detected signals was probably caused by the too much loading of poorly-conductive proteins on the electrode. Thus, the optimal concentration of gelsolin was set as

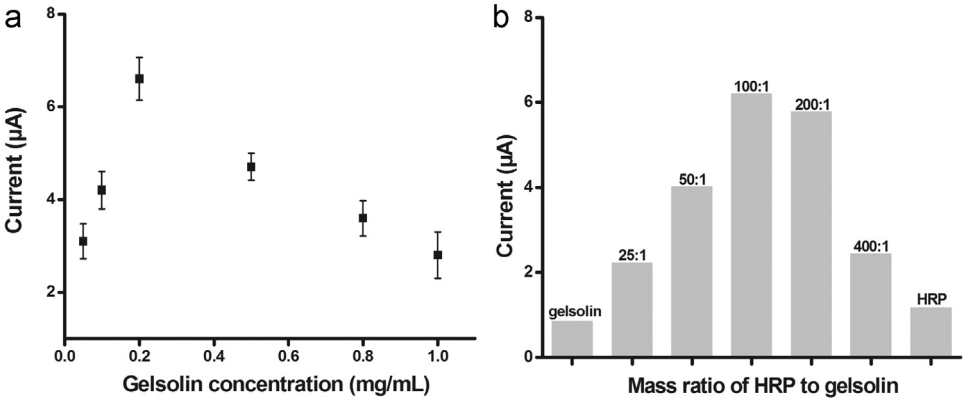

Fig. 2. Effects of (A) gelsolin concentration (from 0.05 to 1.0 mg/mL) and (B) mass ratio of HRP to gelsolin on the current magnitudes.

0.2 mg/mL. HRP was employed as the tracer enzyme in the electrocheimcal assay for signal generation and amplification whereas gelsolin acted as the recognition element for capturing the targets. Due to the intrinsic property of high surface-to-volume ratio, AuNPs could afford a mass of HRP molecules with a relatively low content of gelsolin by controlling the mass ratio of HRP to gelsolin during preparation of the conjugate and observing the change of the reduction peak currents upon the increasing ratios. As shown in Fig. 2B, the influence of the mass raito between HRP and gelsolin on the signal displayed an inverted-V shape, which was initially increased with the increasing mass ratio of HRP to gelsolin until the maximum value appeared at 100:1, followed by a sharp decrease, indicative of the insufficient binding sites on the conjugate to recognize Aβ due to the low amount of gelsolin. As a result, 100:1 was selected as the optimal mass raito of HRP to gelsolin and applied for the preparation of the conjugate.

3.5. Sensitivity, reproducibility and stability of the proposed electrochemical assay

To assess the sensitivity of the proposed electrochemical assay, routine samples of Aβ with different concentrations using the developed sandwich-type format were measured. As demonstrated in Fig. 3, the DPV peak currents (i_p) increased with the increment of Aβ concentrations in the standard sample solution after the incubation. Under the optimal conditions, the current signals were proportional to Aβ concentrations in the range of 0.1–50 nM with a correlation coefficient R of 0.991. The limit of detection (LOD) was approximately 28 pM, which was calculated according to IUPAC recommendations (IUPAC, 1976), LOD$=3S_b/m$, where S_b is the standard deviation of the intercept ($n=11$), and m is the slope value of the respective calibration graph (Wang et al., 2014). This LOD value was equal to or better than that of other reported $A\beta_{1-40/1-42}$ assays (Ammar et al., 2013; Picou et al., 2010; Wang et al., 2012; Xia et al., 2010), illustrating an enhanced sensitivity. Moreover, as the physiological level of $A\beta_{1-40/1-42}$ in rat brains falls within nanomoar levels, the lower LOD is promising to real sample determination. As a control, another HRP–gelsolin bioconjugate without AuNPs for protein enrichment was designed. Under the same optimal conditions, the change of current was slight upon the increasing peptide concentrations (inset in Fig. 3), falling 96% in sensitivity relative to that of HRP–Au–gelsolin, indicating the superority of the proposed strategy. The obtained precision of the methodology with relative standard deviations of 1.75% for intra-day and 3.03% for inter-day precision ($n=8$) indicated the satisfactory reproducibility, which was similar or suprior to that for other assays (Liu et al., 2013; Xia et al., 2010). After the sensor was stored in dry at 4 °C for two weeks, 90% of its initial current response was retained, which further demonstrated an acceptable reliability and stability of the detection signal using the fabricated assay (Fig. S4).

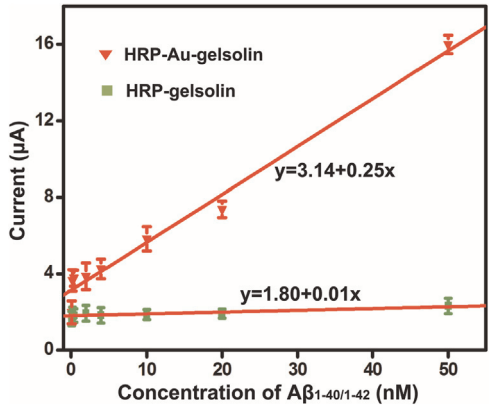

Fig. 3. Linear plots of DPV peak currents at +0.35 V (*vs.* SCE) as a function of $A\beta_{1-40/1-42}$ concentrations (0.1, 0.2, 0.4, 2, 4, 10, 20, 50 nM) using the prepared HRP–Au–gelsolin and HRP–gelsolin as probes, respectively.

3.6. Electrochemical evaluation of brain $A\beta_{1-40/1-42}$ levels

As demonstrated above, the developed electrochemical assay for $A\beta_{1-40/1-42}$ evaluation, featuring high sensitivity and selectivity, provided a reliable *in vivo* platform for $A\beta_{1-40/1-42}$ sensing in both normal and AD rat brains. In this application, construction of a credible AD model is a key issue related to the following analysis. Recent studies in our laboratory have shown that D-galactose administration (i.p.) and bilateral ibotenic acid (IBO) injection into NBM (nucleus basalis magnocellularis) could cause the neurodegeneration and change the levels of neuropeptides in rat brain. And we have also confirmed the success in the modeling of early AD rats through a series of molecular biology techniques (Yu et al., 2014).

Fig. 4A and B displays the electrochemical responses obtained at the fabricated detection assay in CSF and brain tissues (hippocampus, prefrontal cortex and striatum) sampled from normal (A) and AD (B) rats. As was seen, the DPV responses from CSF and brain tissues differed greatly between normal and AD rats, indicating the variations in the levels of $A\beta_{1-40/1-42}$ associated with AD. According to the calibration results, the concentrations of $A\beta_{1-40/1-42}$ in these above brain areas of rats with AD were in the range of 5.20–9.30 nM (Table 1), which was similar to our previous results. A representative 3D plot describing the levels of $A\beta_{1-40/1-42}$ distributed in both normal and AD rats as well as the level variations induced by aggregations of Aβ associated with AD process was illustrated in Fig. 4C. A clear decline in the concentration of soluble $A\beta_{1-40/1-42}$ in these brain regions of AD rats was observed compared with that in normal group due to the aggregations of these peptides as AD progresses, which was in good aggreement with previous observations that $A\beta_{1-40/1-42}$ aggregation in AD occurs not only in CSF but also in brain tissues (Ikonomovic et al., 2008; Strozyk et al., 2003). Among these regions, the reduction in soluble $A\beta_{1-40/1-42}$ monomer levels was greatest in CSF, followed by hippocampus, cortex and striatum, a tendency consistent with our foregoing findings. The concept of the primary role of Aβ in AD neuropathology has been reinforced by the well-established Aβ accumulation in the brains of AD sufferers (Borchelt et al., 1996). The peptide accumulation is a progressive course, in which a key event of changes in the morphology of Aβ are involved, from its soluble monomeric form into oligomers and fibrillated aggregates in the brain (Jiang et al., 2012), thus reduces the amount of soluble $A\beta_{1-40}$ and $A\beta_{1-42}$ monomers in brain. It should be highlighted that this work innovatively realized the assessment of Aβ levels both in CSF and three brain tissues sampled from AD rats, which was more comprehensive and reliable to understand the pathogenesis of this neurodegenerative disease than those that focused only on CSF determination, as we mentioned above that the peptide aggregation in AD occurs not only in CSF but also in brain tissues.

The detected results of $A\beta_{1-40/1-42}$ in rat brain by the developed method were also compared with those obtained using commercial $A\beta_{1-40}$ and $A\beta_{1-42}$ ELISA technique. As summaried in Table 1, although the absolute concentrations determined with the two assays were different, both assays revealed a similar trend of the decrease in $A\beta_{1-40/1-42}$ levels in AD rats compared with normal group, that was decrease in soluble $A\beta_{1-40/1-42}$ monomer levels was greatest in CSF, followed by hippocampus, prefrontal cortex and striatum. The bias in the absolute concentration of Aβ between a newly-developed method and a proprietary ELISA has been reported, which could be attributed to the self aggregations

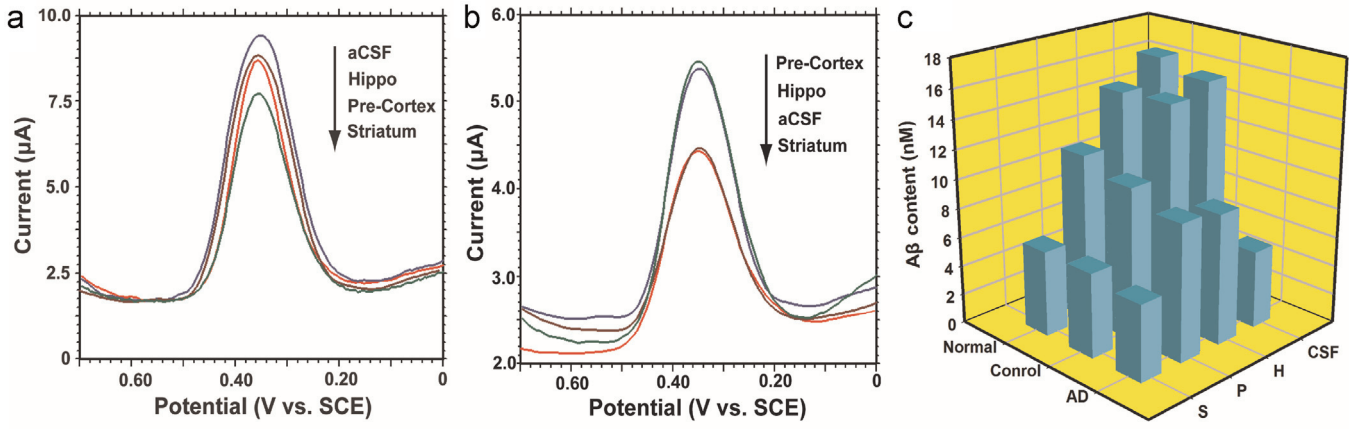

Fig. 4. DPV responses of $A\beta_{1-40/1-42}$ in normal (A) and AD (B) rats on the gelsolin-bound-$A\beta_{1-40/1-42}$ detection assay. (C) A representative 3D illustration for the level changes of $A\beta_{1-40/1-42}$ in CSF, hippocampus, prefrontal cortex and striatum of normal, control and AD rats. S, P, and H represent striatum, prefrontal cortex and hippocampus, respectively.

Table 1
Results of the determination of $A\beta_{1-40/1-42}$ in CSF and brain tissues from normal and AD rats using the proposed electrochemical detection assay and ELISA (mean ± S.D., $n=8$).

$A\beta_{1-40/1-42}$ concentration (nM)	Animal group	CSF	Hippocampus	Prefrontal cortex	Striatum
Present method	Normal	16.56 ± 2.46	14.88 ± 1.56	11.42 ± 1.94	5.84 ± 0.81
	Control	15.79 ± 0.87	15.03 ± 1.33	10.4 ± 0.69	5.77 ± 0.34
	AD	5.28 ± 0.64	8.88 ± 0.98	9.30 ± 1.21	5.20 ± 0.56
ELISA	Normal	12.25 ± 3.09	12.83 ± 1.66	7.58 ± 0.85	6.01 ± 1.96
	Control	11.86 ± 2.62	13.35 ± 2.19	8.12 ± 2.31	4.91 ± 1.12
	AD	3.72 ± 0.74	6.85 ± 1.36	6.08 ± 1.68	5.47 ± 1.53

of Aβ related to different assay conditions (Shin et al., 2014; Watanabe et al., 2012). This comparison signifies that the developed electrochemical assay based on the specific binding between Aβ and gelsolin opened up a a reliable *in vivo* approach for determining the concentrations of Aβ in rat brain, as well as further investigating the role of this important biomarker played in AD progress.

4. Conclusions

In summary, combining the unique and high affinity of gelsolin and $A\beta_{1-40/1-42}$, the proposed gelsolin-bound-$A\beta_{1-40/1-42}$ detection assay has been accomplished for detecting level variations of $A\beta_{1-40/1-42}$ associated with AD progress. With signal amplification by a bioconjugate formed between AuNPs and HRP, as low as 28 pM $A\beta_{1-40/1-42}$ can be readily measured, which is therefore reliably transferable to evaluate soluble $A\beta_{1-40/1-42}$ contents in both CSF and brain tissues of normal and AD rats, thus providing a useful tool to study the changes that occur in neurodegenerative diseases. We believe that the simplicity, sensitivity, and selectivity of this assay would make it potentially suitable for the early and clinical diagnosis of human AD patients.

Acknowledgment

We greatly appreciate the Program of the National Natural Science Foundation of China (No. 21205102). This work was also sponsored by Qinglan Project and the Priority Academic Program Development of Jiangsu Higher Education Institutions (PAPD).

Appendix A. Supplementary material

Supplementary data associated with this article can be found in the online version at http://dx.doi.org/10.1016/j.bios.2014.12.041.

References

Ammar, M., Smadja, C., Phuong, L.G.T., Azzouz, M., Vigneron, J., Etcheberry, A., Taverna, M., Dufour-Gergam, E., 2013. Biosens. Bioelectron. 40, 329–335.
Bennett, D.A., Schneider, J.A., Arvanitakis, Z., Kelly, J.F., Aggarwal, N.T., Shah, R.C., et al., 2006. Neurology 66, 1837–1844.
Borchelt, D.R., Thinakaran, G., Eckman, C.B., et al., 1996. Neuron 17, 1005–1013.
Chauhan, V.P.S., Ray, I., Chauhan, A., Wisniewski, H.M., 1999. Biochem. Biophys. Res. Commun. 258 (241–246).
Citron, M., 2010. Nat. Rev. Drug. Discov. 9, 387–398.
Glenner, G.G., Wong, C.W., 1984. Biochem. Biophys. Res. Commun. 120, 885–890.
Golde, T.E., Eckman, C.B., Younkin, S.G., 2000. Biochim. Biophys. Acta 1502, 172–187.
Hardy, J., Selkoe, D.J., 2002. Science 297, 353–356.
Ikonomovic, M.D., Klunk, W.E., Abrahamson, E.E., Mathis, C.A., Price, J.C., Tsopelas, N.D., Lopresti, B.J., Ziolko, S., Bi, W.Z., Paljug, W.R., Debnath, M.L., Hope, C.E., Isanski, B.A., Hamilton, R.L., DeKosky, S.T., 2008. Brain 131, 1630–1645.
IUPAC, 1976. Pure Appl. Chem. 45, 107.
Jiang, L.F., Liao, H.L., Huang, H.M., Zhou, L.X., Li, L., Cheng, S.X., Du, C.Z., 2013. Biol. Trace Elem. Res. 152, 50–56.
Jiang, T., Zhi, X.L., Zhang, Y.H., Pan, L.F., Zhou, P., 2012. Biochim. Biophys. Acta 1822, 1207–1215.
Liu, L., He, Q.G., Zhao, F., Xia, N., Liu, H.J., Li, S.J., Liu, R.L., Zhang, H., 2014. Biosens. Bioelectron. 51, 208–212.
Liu, L., Zhao, F., Ma, F.J., Zhang, L.P., Yang, S.L., Xia, N., 2013. Biosens. Bioelectron. 49, 231–235.
Lu, X.M., Tnan, H.Y., Korgel, B.A., 2008. Chem. Eur. J. 14, 1584–1591.
Munishkina, L.A., Fink, A.L., 2007. Biochim. Biophys. Acta 1768, 1862–1885.
Niva, C., Parkinson, J., Olsson, F., Schaick, E.V., Lundkvist, J., Visser, S.A.G., 2013. Eur. J. Clin. Pharmacol. 69, 1247–1260.
Picou, R., Moses, J.P., Wellman, A.D., Kheterpal, I., Douglass Gilman, S., 2010. Analyst 135, 1631–1635.
Rama, E.C., González-García, M.B., Costa-García, A., 2014. Sensor. Actuat. B: Chem. 201, 567–571.
Ranjini, K.S., Chinnaswamy, K., Stanley, S., Pazhani, S., 2012. Int. J. Pept. Res. Ther. 18, 99–106.

Rodrigue, K.M., Kennedy, K.M., Park, D.C., 2009. Neuropsychol. Rev. 19, 436–450.
Selkoe, D.J., 1996. J. Biol. Chem. 271, 18295–18298.
Shin, Y.G., Hamm, L., Murakami, S., Buirst, K., Buonarati, M.H., Cox, A., Regal, K., Hunt, K.W., Scearce-Levie, K., Watts, R.J., Liu, X., 2014. Arch. Pharm. Res. 37, 636–644.
Strozyk, D., Blennow, K., White, L.R., Launer, L.J., 2003. Neurology 60, 652–656.
Thal, D.R., Capetillo-Zarate, E., Del Tredici, K., Braak, H., 2006. The development of amyloid beta protein deposits in the aged brain. Sci. Aging Knowl. Environ. 2006 (6), re1.
Wang, C., Liu, D., Wang, Z., 2012. Chem. Commun. 48, 8392–8394.
Wang, Q., Song, Y., Chai, Y.Q., Pan, G.Q., Li, T., Yuan, Y.L., Yuan, R., 2014. Biosens. Bioelectron. 60, 118–123.
Watanabe, K., Ishikawa, C., Kuwahara, Hiroshi, Sato, K., Komuro, S., Nakagawa, T., Nomura, N., Watanabe, S., Yabuki, M., 2012. Anal. Bioanal. Chem. 402, 2033–2042.
Xia, N., Liu, L., Harrington, M.G., Wang, J.X., Zhou, F.M., 2010. Anal. Chem. 82, 10151–10157.
Yang, J.L., Pattanayak, A., Song, M., Kou, J.H., Taguchi, H., Paul, S., Ponnazhagan, S., Lalonde, R., Fukuchi, K., 2013. J. Mol. Neurosci. 49, 277–288.
Yu, X., Munge, B., Patel, V., Jensen, G., Bhirde, A., Gong, J.D., Kim, S.N., Gillespie, J., Gutkind, J.S., Papadimitrakopoulos, F., Rusling, J.F., 2006. J. Am. Chem. Soc. 128, 11199–11205.
Yu, Y.Y., Zhang, L., Li, C.L., Sun, X.Y., Tang, D.Q., Shi, G.Y., 2014. Angew. Chem. Int. Ed. 53, 12832–12835.
Zhang, S., Xia, J., Li, X., 2008. Anal. Chem. 80, 8382–8388.